

SMUHEP 96-05

hep-lat/9605041

May 1996

The Deconfinement Transition on Coarse Lattices

D. W. Bliss,^a K. Hornbostel,^b G. P. Lepage^c

^aUniversity of California, San Diego, CA 92093

^bSouthern Methodist University, Dallas, TX 75275

^cNewman Laboratory of Nuclear Studies, Cornell University, Ithaca, NY 14853

Abstract

We compute the critical temperature T_c for the deconfinement transition of pure QCD on coarse lattices, with $N_t = 2, 3, 4$, and lattice spacings from .33 fm to .15 fm. We employ a perturbatively improved gluon action designed to remove order a^2 and $\alpha_s a^2$ errors. We find that T_c in units of the charmonium 1P–1S splitting and the torelon mass is independent of a to within approximately 5%.

PACS number(s): 12.38.Gc, 11.10.Wx, 12.38.Mh, 11.10.Gh, 05.70.Fh

1 Introduction

Recent calculations using improved lattice actions have demonstrated in several systems that accuracies of several per cent could be achieved with lattice spacings a as large as half a fermi. Use of an improved gluon action designed to remove order a^2 and $\alpha_s a^2$ errors demonstrated rotational invariance for the static quark potential independent of spacing errors to within 5% on lattices with $a = .4$ fm [1]. Heavy quarkonium simulations with a nonrelativistic action corrected for order v^2 relativistic effects and a^2 errors produced masses with systematic errors as low as 5 MeV [2, 1]. Other applications have included glueballs [3], B mesons [4], light fermions [5, 6] and QCD at high temperatures [7].

The cost of lattice simulations typically increase as $1/a^6$; improving accuracy by decreasing a rapidly becomes prohibitively expensive. An attractive alternative is to add effective interactions to remove spacing errors directly in the lattice action, bringing it closer to the continuum [8]. The use of tadpole-improvement for the link variables and renormalized lattice perturbation theory in the design of these interactions are essential ingredients in these recent successes [9]. Because these corrections can be computed perturbatively, parameters need not be tuned, nor new ones introduced beyond those of continuum QCD [10].

The efficiency with which improved actions remove lattice errors dramatically increases the range of calculations accessible to currently available resources. In this work we employ an improved gluon action to compute the deconfinement temperature of QCD. In addition to its intrinsic importance as a fundamental nonperturbative prediction, it provides an excellent quantity with which to test the accuracy of this and other improvement schemes [11, 12, 13].

2 Improved Gluon Action

We used the improved action of Ref. [14, 15, 1],

$$\begin{aligned} S[U] = & \beta_{\text{pl}} \sum_{\text{pl}} \frac{1}{3} \text{Re Tr}(1 - U_{\text{pl}}) \\ & + \beta_{\text{rt}} \sum_{\text{rt}} \frac{1}{3} \text{Re Tr}(1 - U_{\text{rt}}) + \beta_{\text{pg}} \sum_{\text{pg}} \frac{1}{3} \text{Re Tr}(1 - U_{\text{pg}}) , \end{aligned} \quad (1)$$

with U_{pl} the Wilson loop about a single plaquette, U_{rt} a loop around a 1×2 rectangle, and U_{pg} a parallelogram with links running along the opposing edges of a cube. These terms are sufficient to provide the dimension four and six operators needed for an effective action accurate to order a^4 .

The coefficient β_{pl} is the only input parameter, while

$$\beta_{\text{rt}} = -\frac{\beta_{\text{pl}}}{20 u_0^2} (1 + 0.4805 \alpha_s), \quad \beta_{\text{pg}} = -\frac{\beta_{\text{pl}}}{u_0^2} 0.03325 \alpha_s \quad (2)$$

were computed in terms of β_{pl} using tadpole-improved perturbation theory [16]. The division of each link by u_0 gives tadpole-improved operators. These ensure that the connection between these quantities and their continuum equivalents are not ruined by large tadpole contributions, and are essential for the effectiveness of lattice perturbation theory and the improved action [9]. The measured expectation value of the plaquette determines both u_0 and the renormalized coupling constant α_s self-consistently, with

$$u_0 = \left(\frac{1}{3} \text{Re Tr} \langle U_{\text{pl}} \rangle \right)^{1/4}, \quad \alpha_s = -\frac{\ln \left(\frac{1}{3} \text{Re Tr} \langle U_{\text{pl}} \rangle \right)}{3.06839}. \quad (3)$$

3 Deconfinement Transition and Critical Temperature

Green's functions computed on a Euclidean lattice periodic in time with finite extent t are equivalent to those at the finite temperature $T = 1/t$, averaged with the usual Boltzmann weight $\exp(-H/T)$. In particular, the correlation of a Polyakov loop or Wilson line,

$$P(\mathbf{x}) \equiv \text{Tr} \prod_t^{N_t} U_{(\mathbf{x},t),\hat{t}}, \quad (4)$$

which wraps around the lattice in the time direction, and its adjoint are related to the free energy $F_{Q\bar{Q}}$ of a static quark-antiquark pair separated by \mathbf{x} according to

$$\langle P(\mathbf{x}) P^\dagger(0) \rangle \propto \exp(-F_{Q\bar{Q}}/T). \quad (5)$$

At large separation, cluster decomposition requires

$$\langle P(\mathbf{x}) P^\dagger(0) \rangle \longrightarrow |\langle P(0) \rangle|^2. \quad (6)$$

In the confining phase, $F_{Q\bar{Q}}$ increases with $|\mathbf{x}|$ and $\langle P(0) \rangle$ must therefore vanish; in the deconfined phase, P may acquire a nonvanishing expectation value. Pure SU(3) lattice gauge theory, including improved actions, possesses a global symmetry under multiplication of timelike links at a single time slice by the elements of the group center, Z_3 . Nonzero $\langle P \rangle$ indicates the breakdown of this symmetry. Therefore $\langle P \rangle$ is a suitable and relatively simple order parameter with which to study this transition [17].

As the temperature exceeds its critical value T_c , the system moves from confined to deconfined phases. Measurements of P , which were clustering around zero, now cluster about the real axis, or to the two axes along the other Z_3 elements, $\exp(\pm i2\pi/3)$. During the transition, the system will fluctuate between phases. We determine T_c by the location of the peak in the susceptibility

$$\chi \equiv N_s^3 (\langle P^2 \rangle - \langle P \rangle^2) \quad (7)$$

which measures the deviation in $\langle P \rangle$ these fluctuations induce. Here P is averaged over spatial lattice sites.

Because the volume is finite, the transition temperature is smeared, limiting the precision with which we may determine T_c . Also, above T_c , given sufficient simulation time the system will tunnel between the three degenerate vacua, and $\langle P \rangle$ will still average to zero. It is therefore useful in practice to fold these three axes together [18, 11], replacing P in Eq. (7) with Ω , such that

$$\Omega \equiv \begin{cases} \text{Re } P & ; \arg P \in (-\pi/3, \pi/3) \\ \text{Re } P e^{i2\pi/3} & ; \arg P \in (\pi, -\pi/3) \\ \text{Re } P e^{-i2\pi/3} & ; \arg P \in (\pi/3, \pi) . \end{cases} \quad (8)$$

We move our lattice system through the phase transition by holding $N_t = 1/aT$ fixed while adjusting β_{pl} , and therefore implicitly the lattice spacing a . We are measuring a quantity defined at infinite spatial volume, and N_t should be small relative to the number of spatial sites per side, N_s . We determined β_{pl}^c on lattices with $(N_s^3 \times N_t)$ of $(4^3 \times 2)$, $(6^3 \times 2)$, $(6^3 \times 3)$, $(9^3 \times 3)$ and $(8^3 \times 4)$.

After determining the critical coupling β_{pl}^c at which the transition occurs, we computed a convenient mass M with this same β_{pl}^c but at zero temperature, with $N_t > N_s$. The value of Ma from this simulation fixes a , and therefore T_c , in units of M . Comparison with data for M gives T_c in physical units. We chose for M the charmonium $1P - 1S$ splitting, and also the

torelon mass, which is related to the string tension.

To determine β_{pl}^c , we began with β_{pl} below transition and used one thousand Metropolis updates to allow the lattice to thermalize. We then sampled the Polyakov loop after every five updates for the next one or two thousand. After stepping β_{pl} up and allowing several hundred more updates, we began sampling again, repeating until β_{pl} had crossed its critical value. To ensure that the number of updates was sufficient to thermalize, we stepped β_{pl} back down through the transition to check for hysteresis.

Figs. 1 through 5 display the susceptibility plots for each lattice as a function of β_{pl} . The up and down arrows indicate data from upward and downward sweeps. The solid and dashed lines show independent fits of each to a Gaussian and a first order polynomial. The error bars indicate bootstrap estimates. We determine β_{pl}^c from the location of the peak, and assign the Gaussian width as the error. Table 1 presents the weighted average of β_{pl}^c for each T_c .

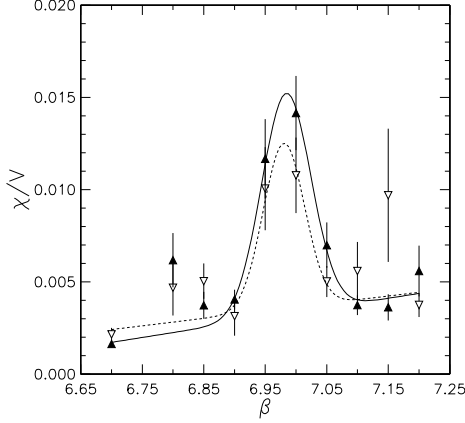


Figure 1: Susceptibility χ for $4^3 \times 2$ lattice. Arrows indicate upward or downward sweeps of β_{pl} through transition.

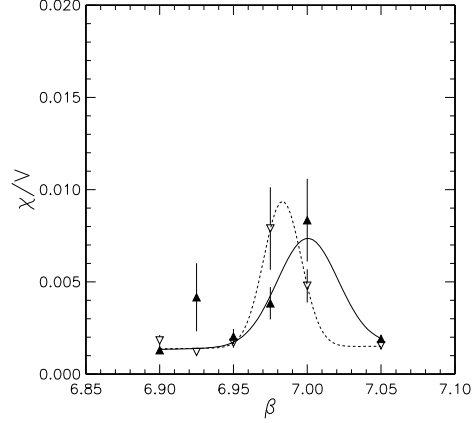


Figure 2: χ for $6^3 \times 2$ lattice.

While we found locating the peak in χ the most reliable method for locating β_{pl}^c , an alternative is to locate the phase change by directly observing

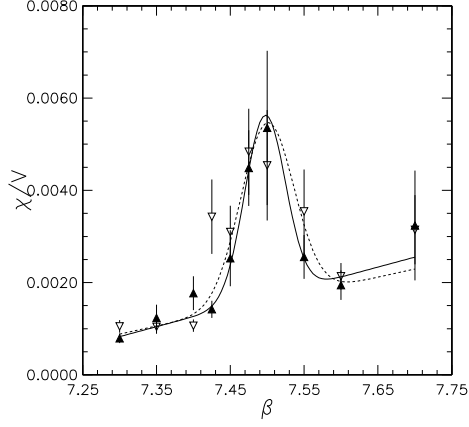


Figure 3: χ for $6^3 \times 3$ lattice.

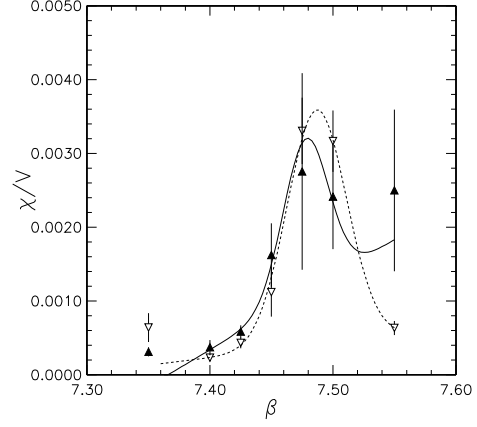


Figure 4: χ for $9^3 \times 3$ lattice.

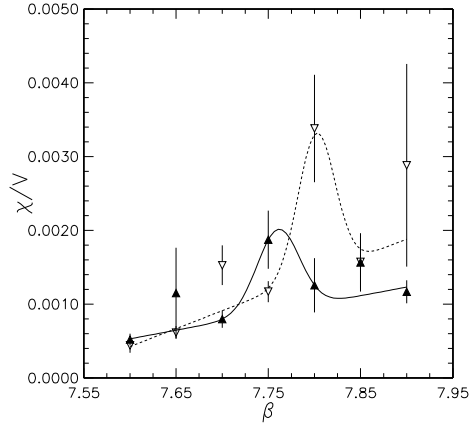


Figure 5: χ for $8^3 \times 4$ lattice.

T_c	1/2	1/3	1/4
β_{pl}^c	6.99(1)	7.49(1)	7.78(2)

Table 1: Critical coupling β_{pl}^c as a function of critical temperature. T_c is in lattice units.

P as a function of β_{pl} . Ref. [19] implements this by choosing a threshold in the fraction of $\langle P \rangle$'s found near any Z_3 axis. Fig. 6 displays the real and imaginary parts of P measured during an upward sweep of β_{pl} on the $9^3 \times 3$ lattice. The transition is evident. Below β_{pl} of about 7.45, P clusters about the origin. During the transition it explores the three degenerate vacua which break Z_3 , before settling into one above the transition. Given sufficient simulation time, P will populate each arm equally. In our study, it rarely explored more than two of the three.

4 Charmonium

To test the dependence of these results on the lattice spacing and to convert the critical temperatures to physical units, we computed the mass difference M_{PS} between the $1P$ and $1S$ states of charmonium on lattices with the same spacings at zero temperature. We chose this quantity because it is experimentally well-measured, simple to compute accurately using a nonrelativistic action (NRQCD) [20, 2], small and therefore insensitive to finite lattice errors, and its splittings are essentially independent of the charm quark mass. We used an NRQCD quark action which removes the leading order a^2 and v^2 errors in lattice spacing and quark velocity, and so is consistent with the gluon action. The dominant uncorrected error is $\mathcal{O}(a^2 v^2)$, due to the a^2 error in the lattice version of the $\mathbf{D} \cdot \mathbf{E}$ relativistic $\mathcal{O}(v^2)$ correction. We did not include dynamical light quarks. Spin splittings are absent to this order, and we compare our results to spin-averaged data.

Table 2 presents the values for M_{PS} for these lattices. We tuned the charm quark mass M_C by requiring that the energy for states carrying nonzero momentum satisfy the usual nonrelativistic dispersion relation. Comparing the lattice result to the experimental spin-averaged value for this splitting, $M_{\text{PS}} = 457.9$ MeV, fixes the inverse lattice spacing.

We obtained these masses by 2×2 correlated matrix fits of exponentials to three propagators for which either the source, the source and sink, or neither were smeared by the lattice equivalent of $\exp(-p^2/12) \sim (1 + \nabla^2/12)$, designed to suppress states with large momentum. We fit to both the ground and first excited states in each channel. Including the excited state prevented it and higher states from contaminating the value for the ground state, and allowed us to include data from lower times. We found this procedure useful

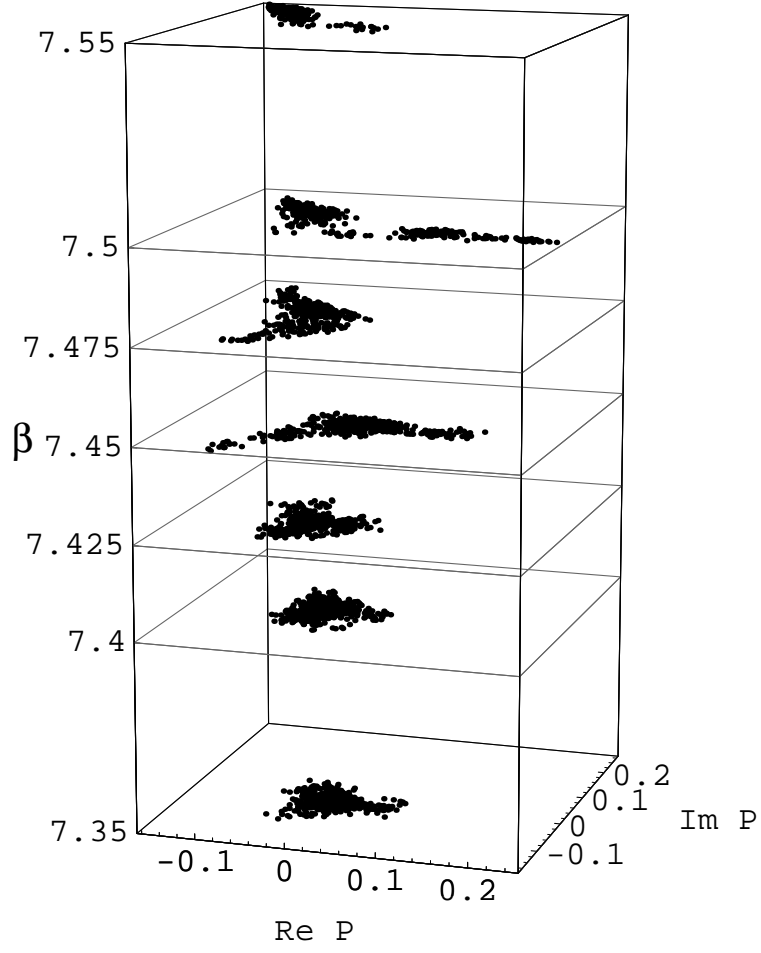


Figure 6: Real and imaginary parts of Polyakov loops measured on a $9^3 \times 3$ lattice, during an upward sweep of β_{pl} through β_{pl}^c .

β_{pl}^c	T_c	lattice	M_C	M_{PS}	a^{-1} [GeV]
6.99	1/2	$3^3 \times 12$	2.0	.77(1)	.596(8)
6.99	1/2	$4^3 \times 12$	2.0	.794(4)	.577(3)
7.49	1/3	$6^3 \times 12$	1.3	.494(6)	.93(1)
7.78	1/4	$6^3 \times 12$.98	.378(7)	1.21(2)
7.78	1/4	$8^3 \times 12$.98	.375(4)	1.22(1)

Table 2: M_{PS} as a function of β_{pl}^c . Errors are statistical. The critical temperature T_c , the charm mass M_C , and the $1P - 1S$ splitting M_{PS} are in lattice units. The experimental value for M_{PS} fixes a .

β_{pl}^c	T_c	lattice	T_c/M_{PS}	T_c [MeV]
6.99	1/2	$3^3 \times 12$.651(14)	298(6)
6.99	1/2	$4^3 \times 12$.630(10)	288(5)
7.49	1/3	$6^3 \times 12$.675(13)	309(6)
7.78	1/4	$6^3 \times 12$.661(17)	303(8)
7.78	1/4	$8^3 \times 12$.667(14)	305(7)

Table 3: Critical temperature T_c in units of M_{PS} and in MeV.

in Ref. [2], and especially helpful in extraction of torelon masses, discussed below. Typically we obtained good fits by including minimum times from 3 to 6, to maximum times from 9 to 12.

Table 3 displays the critical temperature in units of M_{PS} and in MeV, using the experimental value for M_{PS} . Fig. 7 presents the average T_c for each a , around the central value $T_c = 300(6)$ MeV. Along with the statistical errors of quoted for M_{PS} in Table 2, we include errors associated with uncertainties in the critical value for β_{pl} and in the value for the average plaquette u_0 , which is used to tadpole-improve the operators in the action which remove the $\mathcal{O}(a^2)$ errors. To determine the former, we used one-loop perturbative evolution to estimate the variation of M_{PS} with β_{pl} . For the latter, a variation in u_0 would affect the ability of the improved action to remove $\mathcal{O}(a^2)$ errors. We estimated the percentage error by $\delta u_0/u_0$ times the typical (and similar) $\mathcal{O}(a^2)$ errors for these systems: $a^2 \langle p^2 \rangle$ for charmonium,

and $a^2\sigma^2$ for the torelon, discussed below. Here σ is the string tension, and δu_0 the difference between the input and measured value. We found these methods to provide a reasonably reliable estimate of the variation of M_{PS} and the torelon mass in the data over a fairly broad range in β_{pl} and u_0 .

The values for T_c are nearly consistent within these errors, and show little dependence on lattice spacing. We note that values for T_c/M_{PS} for the coarsest lattices ($\beta_{\text{pl}}^c = 6.99$) deviate by about two standard deviations. This is a possible indication of the $\mathcal{O}(a^4)$ systematic errors for which the action is uncorrected. These might be expected to range from about 5–10% for the coarsest lattice (about 1/3 fm) to a couple per cent for the finest (1/6 fm).

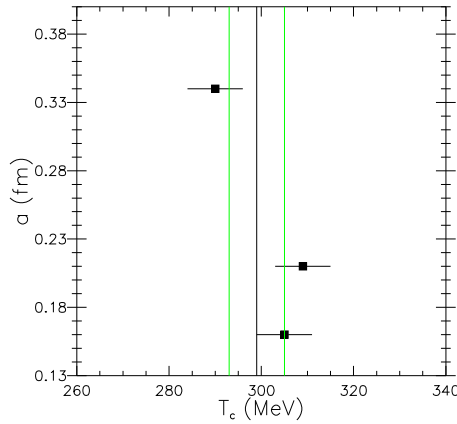


Figure 7: Critical temperature T_c as a function of lattice spacing a , around central value. M_{PS} sets the physical scales.

5 Torelon Mass

As a second test of scaling, we measured the torelon mass μ for torelons of two different physical lengths at these same β_{pl} . The torelon is created by a Wilson loop strung along the full spatial extent of the periodic lattice, and averaged over spatial orientations and transverse positions [21]. As such, it is sensitive to both the string tension σ and lattice length L .

β_{pl}^c	T_c	lattice	μ	μ^*
6.99	1/2	$3^3 \times 12$	1.46(2)	—
6.99	1/2	$4^3 \times 12$	2.26(5)	—
7.49	1/3	$6^3 \times 12$	1.42(1)	3.0(4)
7.78	1/4	$6^3 \times 12$.676(6)	1.8(3)
7.78	1/4	$8^3 \times 12$	1.05(2)	2.1(1)

Table 4: Torelon mass μ and excited torelon mass μ^* vs. β_{pl}^c . Errors are statistical. T_c is the critical temperature in lattice units.

We obtained the torelon mass from the exponential decay in the correlation between two such loops at different times. More precisely, we accounted for periodicity in time by fitting to hyperbolic cosines rather than exponentials, and typically fit to time steps from one to six. For sufficient length L , the mass should go as

$$\mu \sim \sigma L, \quad (9)$$

reflecting the cost in energy of keeping static charges separated by this distance. We will use μ to determine a value for σ below.

We may estimate the energy expected for excited states by comparing to those of a classical vibrating periodic string, $2\pi n/L$. This would suggest first excited states split from the ground states by $2\pi/N_s$ in lattice units, close to the values we observe. For larger lattices, it therefore becomes increasingly important to include these states in fits.

To extract the torelon masses, we performed correlated 3×3 matrix fits of three hyperbolic cosines to six torelon propagators which were smeared once, twice or unsmeared at either the source or sink. To smear these, we used the operator $\exp(-\alpha p_\perp^2)$ on the link variables [22], which suppressed contributions with large momentum transverse to the loop. Specifically, we applied n times the lattice version of $(1 + \alpha \nabla_\perp^2/n)$, with n typically 7 and 14, and α effectively .6 and 1.2. We reunitarized the link variables between applications.

Table 4 lists the results of these fits for the ground state masses and several of the excited states. For smaller lattices, we were unable to get accurate fits for the excited states, presumably due to the larger splitting,

β_{pl}^c	T_c	L	T_c/μ	T_c/μ^*	μ/M_{PS}	μ^*/M_{PS}
6.99	1/2	3	.343(7)	—	1.79(4)	—
7.78	1/4	6	.370(7)	.139(23)	1.90(4)	4.8(8)
6.99	1/2	4	.221(6)	—	2.78(8)	—
7.49	1/3	6	.235(4)	.111(14)	2.87(4)	6.1(8)
7.78	1/4	8	.238(6)	.119(6)	2.85(6)	5.6(3)

Table 5: Critical temperature T_c in units of the torelon masses μ and μ^* , and the ratio of these to M_{PS} . Entries are grouped according to torelons of the same physical length L , given in lattice units.

β_{pl}^c	T_c	L	L [fm]	σa^2	$\sqrt{\sigma}L$	$T_c/\sqrt{\sigma}$	$\sqrt{\sigma}$ [MeV]
6.99	1/2	3	.99(2)	.603(1)	2.33(2)	.644(5)	463(8)
7.78	1/4	6	.98(3)	.142(2)	2.26(2)	.664(5)	456(9)
6.99	1/2	4	1.37(2)	.631(15)	3.18(4)	.630(7)	458(8)
7.49	1/3	6	1.28(2)	.266(4)	3.09(2)	.647(5)	478(6)
7.78	1/4	8	1.29(3)	.148(4)	3.07(4)	.651(8)	469(6)

Table 6: String tension σ defined by Eq. (10), given in the dimensionless combinations with T_c and L , and in MeV. M_{PS} fixes the physical scales.

and settled for 2×2 matrix fits to two hyperbolic cosines. Our ground state masses μ fell below those of Ref. [12], from 3% below at $T_c = 1/2$, increasing to 12% below for $T_c = 1/4$. This may indicate excited state contamination in their fits, which would account for the increasing discrepancy with torelon length. We did reproduce their result for the torelon on a $3^3 \times 16$ lattice using an unimproved Wilson action at $\beta = 5.10$, obtaining 1.82(3), which we computed as a check. In this case we were unable to reliably fit the excited state or include time steps much beyond the first couple.

In Table 5 we present the critical temperature in units of the torelon masses, as well as the ratio of these masses to M_{PS} . The torelons we studied had two different physical lengths, determined by the ratio of L to $1/T_c$, and are grouped accordingly. In most cases, these quantities are independent of a to within statistical errors. There is roughly a 5% discrepancy for the coarsest lattice, which may indicate an $\mathcal{O}(a^4)$ effect. Ref. [12] found about 15% violations for an unimproved Wilson action, while results from their improved (perfect) action scaled within errors.

We define the string tension σ in terms of a torelon of finite length L by

$$\sigma \equiv \mu/L + \pi/(3L^2) , \quad (10)$$

and demonstrate scaling in various dimensionless ratios involving σ in Table 6. The extra Coulombic term in Eq. (10) accounts for long wavelength fluctuations, and appears universally in quantized string models when L is finite [23, 21]. Without it, we found that quantities in the last two columns for the two different physical lengths independently scale, but show a significant discrepancy when compared, providing confirmation for these models. Finally, using M_{PS} to determine the scale, we give values for the string tension in MeV. Central values from these last two columns are $T_c/\sqrt{\sigma} = .649(5)$ and $\sqrt{\sigma} = 467(4)$ MeV.

6 Conclusions

We computed the critical temperature T_c for the pure QCD deconfining transition on coarse lattices, with spacing a from .33 fm to .15 fm. By comparison with charmonium splittings and torelon masses measured at these same spacings, we demonstrated that a gluon action improved to remove $\mathcal{O}(a^2)$ errors could measurements nearly free of lattice spacing errors. In particular, that

lattices with N_s as small as three could give results for T_c accurate to 5%. This precision is consistent with those found previously for charmonium and for the static quark potential. We found central values for T_c and the string tension σ of $T_c = 300(6)$ MeV, $T_c/\sqrt{\sigma} = .649(5)$ and $\sqrt{\sigma} = 467(4)$ MeV.

7 Acknowledgments

We performed many of the simulations on the IBM SP-2 supercomputer at the Cornell Center for Theory and Simulation. This work was supported by grants from the NSF and DOE.

References

- [1] M. Alford, W. Dimm, G. P. Lepage, G. Hockney, and P. B. Mackenzie, Phys. Lett. **B361**, 87 (1995); G. P. Lepage, invited talk at International Symposium on Lattice Field Theory, Melbourne, Australia, 11-15 Jul 1995.
- [2] C. T. H. Davies, K. Hornbostel, A. Langnau, G. P. Lepage, A. Lidsey, J. Shigemitsu, and J. Sloan, Phys. Rev. D **50**, 6963 (1994); C. T. H. Davies, K. Hornbostel, G. P. Lepage, A. Lidsey, J. Shigemitsu, and J. Sloan, Phys. Rev. D **52**, 6519 (1995).
- [3] C. Morningstar and M. Peardon, invited talk at International Symposium on Lattice Field Theory, Melbourne, Australia, 11-15 Jul 1995.
- [4] S. Collins, U. M. Heller, J. H. Sloan, J. Shigemitsu, A. Ali Khan and C. T. H. Davies, preprint FSU-SCRI-96-13, Feb 1996.
- [5] M. Alford, T. Klassen and G. P. Lepage, invited talk at International Symposium on Lattice Field Theory, Melbourne, Australia, 11-15 Jul 1995.
- [6] H. R. Fiebig and R. M. Woloshyn, preprint TRI-PP-96-1, Feb 1996.
- [7] B. Beinlich, F. Karsch, and E. Laermann, Nucl. Phys. **B462**, 415 (1996).
- [8] K. Symanzik, Nucl. Phys. **B226**, 187 (1983).

- [9] G. P. Lepage and P. B. Mackenzie, *Phys. Rev. D* **48**, 2250 (1993).
- [10] An alternative approach removes all spacing errors; see P. Hasenfratz and F. Niedermayer, *Nucl. Phys.* **B414**, 785 (1994).
- [11] G. Cella, G. Curci, A. Viceré, and B. Vigna, *Phys. Lett.* **B333**, 457 (1994).
- [12] T. DeGrand, A. Hasenfratz, P. Hasenfratz, and F. Niedermayer, *Nucl. Phys.* **B454**, 615 (1995).
- [13] For a recent calculation using an unimproved Wilson action on a large lattice, see G. Boyd, J. Engels, F. Karsch, E. Laermann, C. Legeland, M. Lutgemeier and B. Petersson, preprint BI-TP-96-04, Jan 1996.
- [14] G. Curci, P. Menotti, and G. Paffuti, *Phys. Lett.* **130B** 205 (1983). Erratum: *ibid.* **135B** 516 (1984).
- [15] M. Lüscher and P. Weisz, *Comm. Math. Phys.* **97** 59 (1985).
- [16] These are adapted from results in M. Lüscher and P. Weisz, *Phys. Lett.* **158B**, 250 (1985), and references therein.
- [17] See, for example, B. Svetitsky, *Phys. Rep.* **132**, 1 (1986). M. Creutz, *Quarks, Gluons and Lattices*, Cambridge University Press, Cambridge, 1983. H. J. Rothe, *Lattice Gauge Theories*, World Scientific Publishing Co., Singapore, 1992.
- [18] M. Fukugita, M. Okawa, and A. Ukawa, *Nucl. Phys.* **B337**, 181 (1990);
- [19] N. Christ and A. Terrano, *Phys. Rev. Lett.* **56**, 111 (1986). D. Toussaint, in the *Proceedings of Lattice '86*, H. Satz et al. eds., Plenum, 399 (1987).
- [20] G. P. Lepage, L. Magnea, C. Nakhleh, U. Magnea and K. Hornbostel, *Phys. Rev. D* **46**, 4052 (1992).
- [21] P. de Forcrand, G. Schierholz, H. Schneider, and M. Teper, *Phys. Lett.* **160B**, 137 (1985).
- [22] M. Falcioni, M. Paciello, G. Parisi and B. Taglienti, *Nucl. Phys.* **B251**, 624 (1985). M. Albanese et. al., *Phys. Lett.* **B192**, 163 (1987).

[23] M. Lüscher, K. Symanzik and P. Weisz, Nucl. Phys. **B173**, 365 (1980).